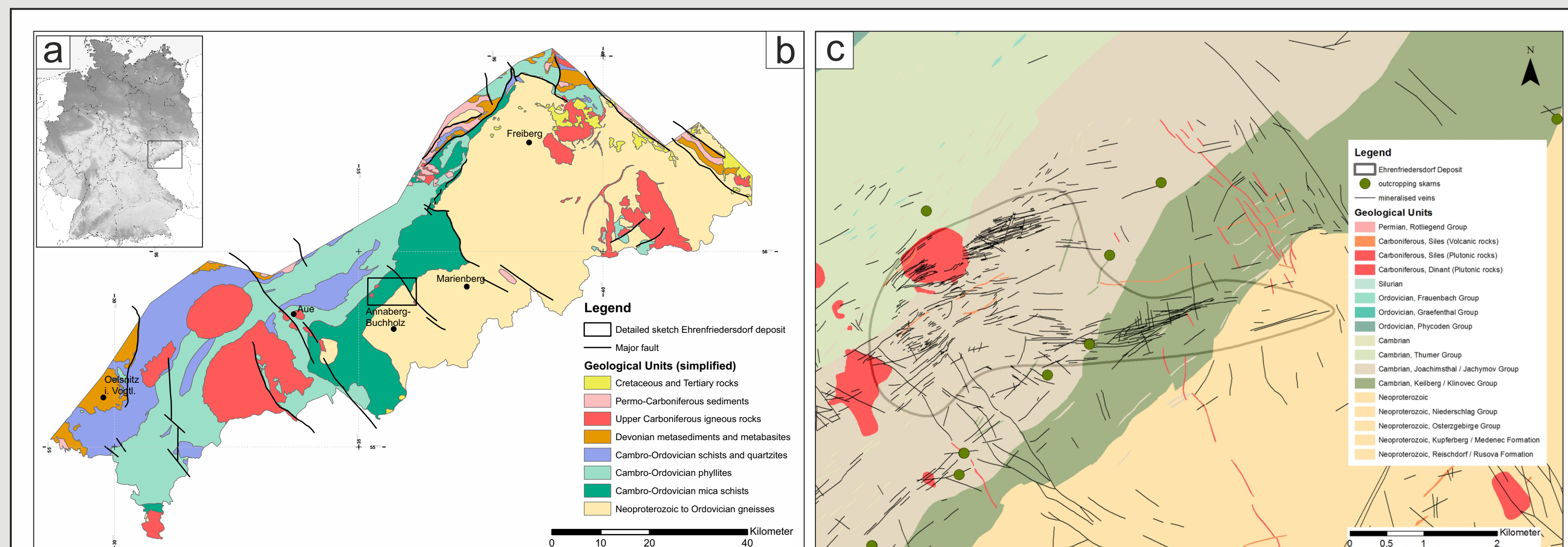


# Petrogenetic investigations of sulfides from polymetallic skarn-type occurrences in the Ehrenfriedersdorf deposit, Germany: Coupled substitution processes of copper-indium in sphalerite

<sup>1</sup>Franke, H., <sup>2</sup>Kallmeier, E., <sup>2</sup>Legler, C., <sup>1</sup>Graupner, T., <sup>1</sup>Schwarz-Schampera, U., <sup>1</sup>Pursche, K

<sup>1</sup>Federal Institute for Geosciences and Natural Resources, Hannover, Germany,

<sup>2</sup>Beak Consultants GmbH, Freiberg, Germany



**Fig. 1:** **a** Location of the Erzgebirge. **b** Schematic geological map of the Erzgebirge (Saxony, Germany) with large historic and recent ore districts, including the main lithologies of the central part of the Saxo-Thuringian zone of the Variscan orogen. **c** Detailed schematic geological map of the Ehrenfriedersdorf district showing the metamorphic rock units, magmatic intrusions and mineralized veins that host the skarn mineralization.

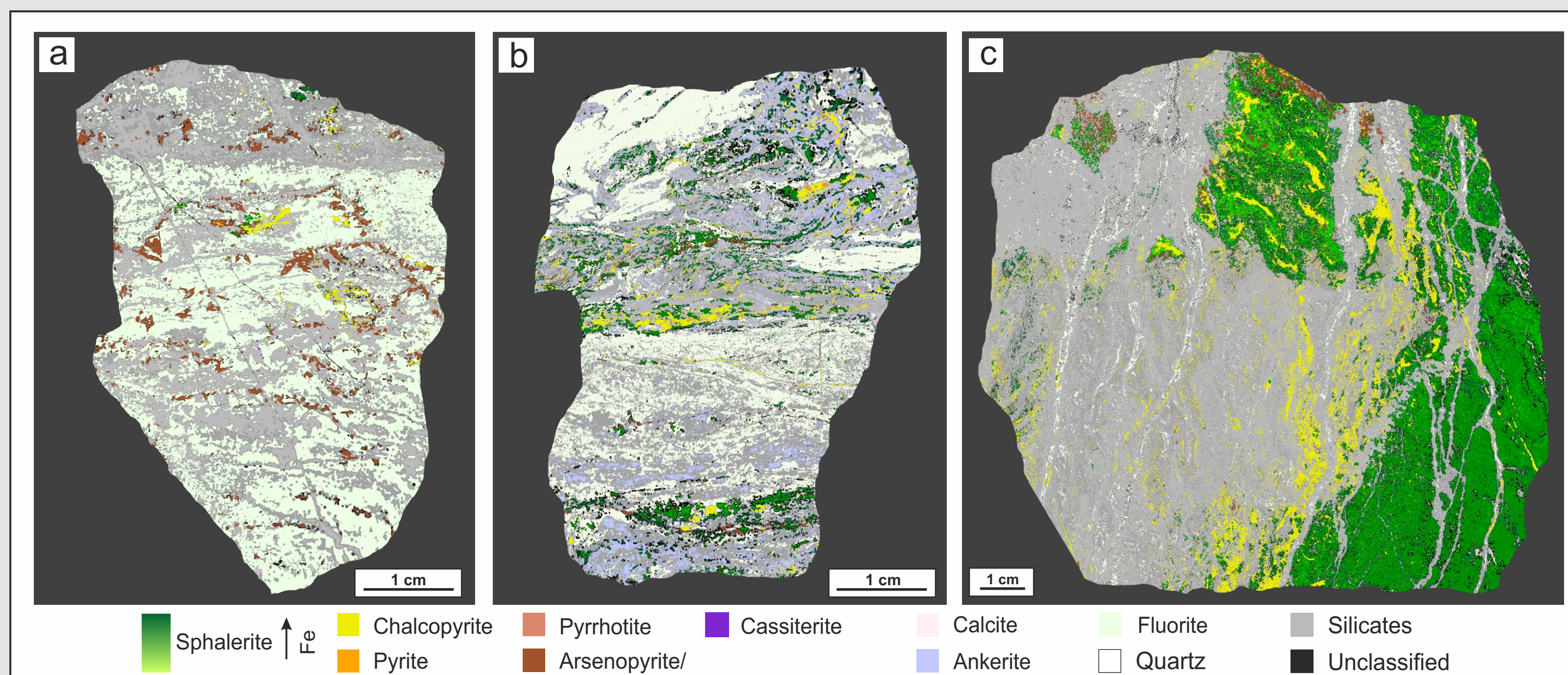


**Fig. 2:**  $\mu$ -EDXRF mineral distribution maps of three representative sulfide samples from the Ehrenfriedersdorf skarn. Sphalerite, chalcocyanite, pyrite, arsenopyrite, loellingite, pyrrhotite and cassiterite are hosted by a suite of silicates, carbonates and fluorite. False color images show different stages of layered sulfide mineralization: **a** arsenopyrite-chalcocyanite-bearing fluorite-actinolite-biotite skarn, **b** fluorite diopside-garnet skarn containing discontinuous stringers of sphalerite-chalcocyanite-pyrite-mineralization with accessory cassiterite and malayaite, and **c** sphalerite-chalcocyanite-dominated sulfide assemblages in pyroxene-amphibole-magnetite skarn.

## Petrographic observations and mineral chemistry

Metasomatism of metacarbonate and metapelite rocks produced calc-silicate hornfels/skarn layers containing pyroxene, amphibole, mica, vesuvianite, calcite, fluorite and rarely malayaite. Layered Sn-rich polymetallic sulfide ores contain mineral assemblages of sphalerite, chalcocyanite, arsenopyrite, loellingite, cassiterite, pyrite, pyrrhotite and rarely scheelite (Fig.2). In this study we focus on the copper-indium distribution in sphalerite and chalcocyanite.

Commonly, medium- to fine-grained sphalerite crystals with up to 0.3 wt.% In and elevated Cu concentrations up to 0.6 wt.% associated with In-poor chalcocyanite show homogeneous compositions in back-scatter-electron images, without any mineral inclusion of roquesite or other indium-bearing mineral phases. However, detailed microscopic observations indicate that one sample of the studied skarn-type rock suite contains three different domains of In enrichment in sphalerite. These are (a) medium- to fine-grained sphalerite I with concentrations up to 0.44 wt.% In and up to 0.3 wt.% Cu next to (b) sphalerite II with In-concentrations up to 4.98 wt.% (< 2.81 wt.% Cu), which include  $\mu$ -scale, crystallographically-orientated lamellae of late-stage roquesite, and (c) sphalerite III associated with two different textures of roquesite. Orientated lamellae at sub- $\mu$ m-scale occur along the crystal planes of sphalerite but also as aggregates with fine-grained irregular crystals next to inclusions of In-rich chalcocyanite (Fig.3; Fig.4). Moreover, EMPA distribution maps show that rims and grain boundaries in sphalerite I are enriched in In up to 1.97 wt.% and Cu with concentrations up to 1.27 wt.%. In contrast nearly all sphalerites contain comparable low Fe concentrations between 0.39 and 1.25 wt.% with an average of 0.72 wt.% (Fig.4) independent of their In or Cu concentrations.

## Conclusion

The petrographic observations and textural evidences indicate late-stage metamorphic and hydrothermal overprinting of the primary sulfidic skarn mineral assemblage by an Cu-In-rich hydrothermal fluid. Described evidences attest to solid state diffusion processes forming so-called chalcocyanite diseases [1] or diffusion-induced segregations [2]. The replacement reactions and exsolution-like phenomena in the low temperature sphalerite reflect that the indium enrichment is related to the coupled substitution of copper and indium with zinc at higher temperatures [3]. Our findings proof the mineralizing fluids to be saturated in indium and copper which is leading the precipitation of roquesite in sphalerite.

### References:

- [1] Barton, P.B., Bethke, P.M. (1987) Chalcocyanite disease in sphalerite: pathology and epidemiology. *American Mineralogist* 72: 451-467.
- [2] Johan, Z. (1988) Indium and germanium in the structure of sphalerite: an example of coupled substitution with copper. *Mineralogy and Petrology* 39: 211-229.
- [3] Bente, K., Doering, Th. (1995) Experimental studies on solid state diffusion of Cu+In in ZnS on a "Disease", DIS (Diffusion Induced Segregations), in sphalerite and their geological applications. *Mineralogy and Petrology* 53: 285-305.

This study contributes to the projects RoStraMet (BGR), HTMET (FKZ 033R131), and WISTAMERZ (FKZ 033R133) funded by the German Government (BMBF).

## Geological setting and sampling

The Erzgebirge represents the central part of the metamorphic basement of the Saxo-Thuringian zone of the Mid-European Variscides. It is located at the NW border of the crystalline Bohemian Massif. The metamorphic rock suite comprises a complex succession of greenschist to amphibolite facies mica schists, gneisses and metacarbonates with peak temperature and pressure values at eclogite facies conditions. Late Carboniferous to early Permian intrusions of late-collisional Variscian granites, subvolcanic dikes, microgranites, and lamprophyres caused metasomatic alteration of the metamorphic rock units and initiated the formation of different magmatic-hydrothermal tin and polymetallic sulfide greisen- and skarn-type deposits.

Samples for this study were provided by BEAK Consultants GmbH and originate from the western area of the Ehrenfriedersdorf deposit, characterized by the occurrence of Sn-bearing skarn-type rock suites. They were investigated by optical microscopy,  $\mu$ -EDXRF, XRD, EMPA and LA-ICP-MS to analyze chemical processes and unravel genetic aspects.

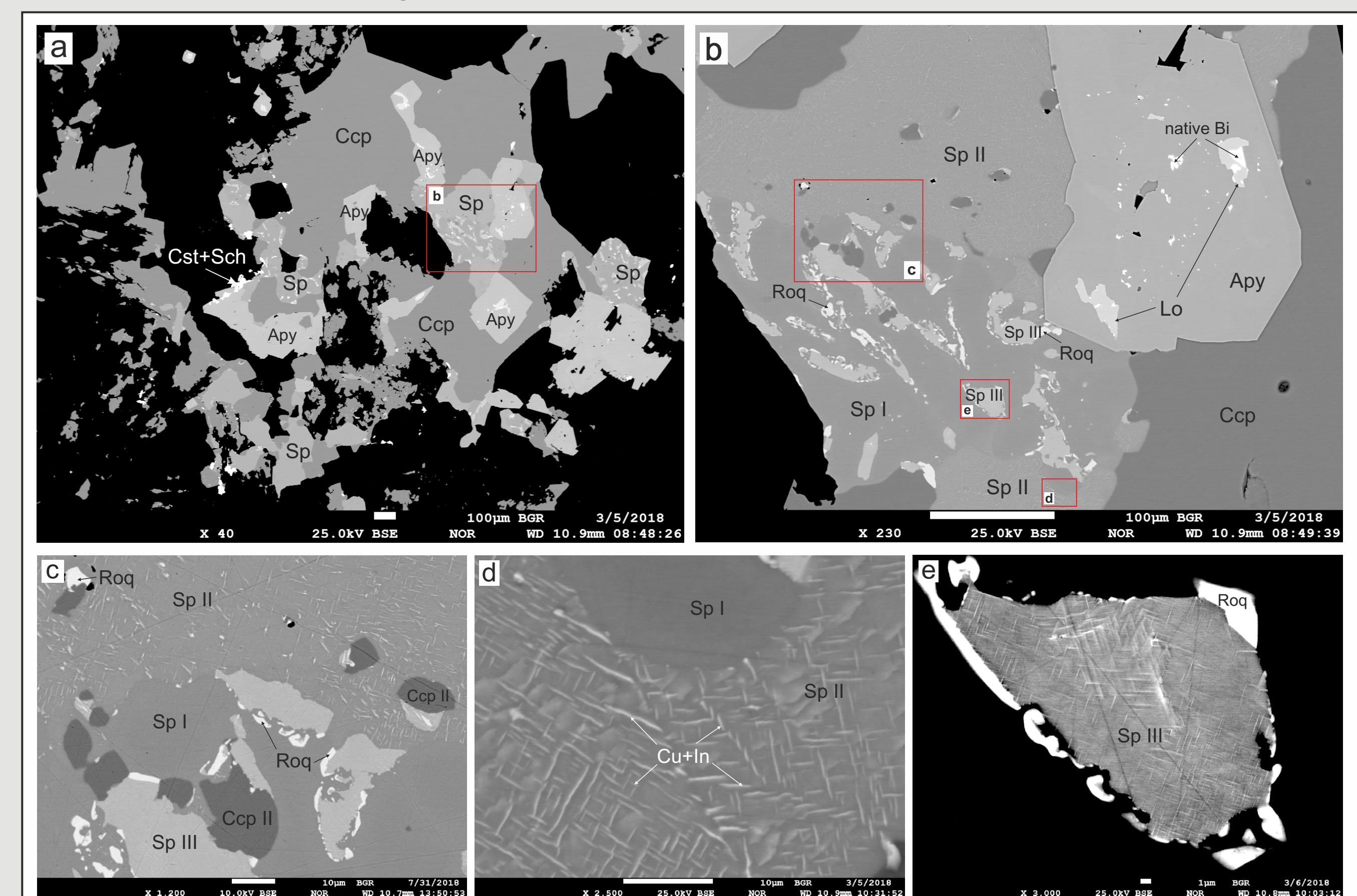


**Fig. 3:** BSE images of the characteristic sulfide assemblage. **a** Chalcocyanite associated with domains of In-bearing sphalerite (Sp), arsenopyrite (Apy), cassiterite (Cst) and scheelite (Sch). **b** Detailed image of Fe-poor sphalerite I (Sp I) with inclusions of sphalerite III (Sp III), roquesite (Roq) and In-bearing chalcocyanite grains next to sphalerite II (Sp II) and associated with arsenopyrite including loellingite (Lo) and native Bi aggregates. **c** Detail of In-rich sphalerite domains containing inclusions of chalcocyanite and roquesite. **d** Border of two sphalerite domains with sphalerite II including orientated lamellae of roquesite at  $\mu$ m scales. **e** Roquesite as inclusion of sub- $\mu$ m-scale lamellae in sphalerite III and as distinct irregular crystals associated with Fe-poor sphalerite I.

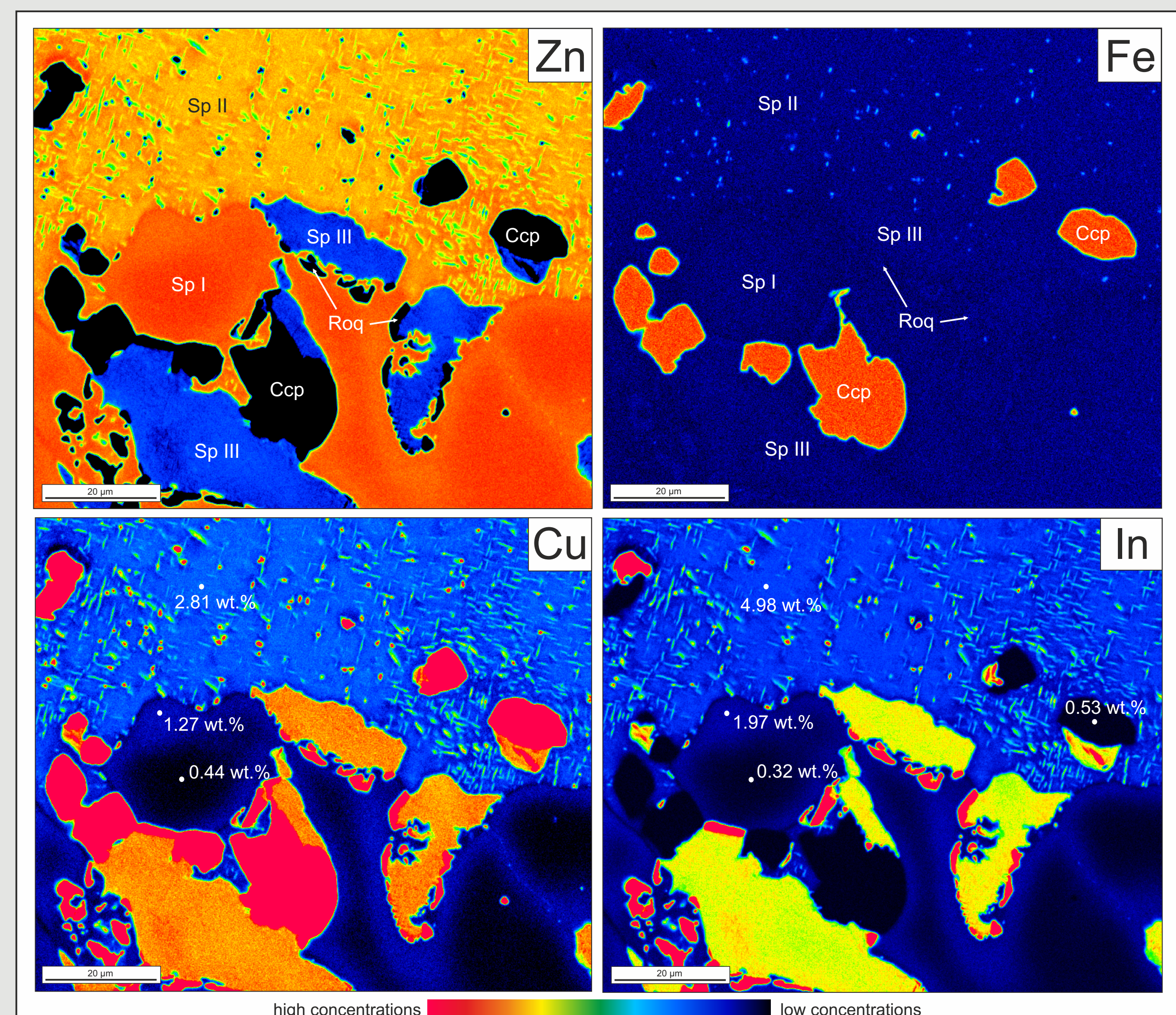


**Fig. 4:** Semi-quantitative high-resolution EMPA element mappings of Zn, Fe, Cu and In (10 kV, 40 nA, 155 ms dwell time) of a sulfide aggregate (Fig.3c) with sphalerite, chalcocyanite and roquesite from skarn-type occurrences of the Ehrenfriedersdorf deposit showing the dispersion of Cu and In diffusion induced segregation processes with precipitation of distinct roquesite (CuInS<sub>2</sub>). White dots mark measuring points with elevated concentrations values. Zn (EDX); Fe, Cu, In (WDX).

### Contact details:

Federal Institute for Geosciences and Natural Resources  
Henrike Franke  
Phone: +49 511 643 2670  
E-mail: henrike.franke@bgr.de  
www.r4-innovation.de